

# Kinetic Analysis of Proton Transport by the Vanadate-Sensitive ATPase from Maize Root Microsomes

David Brauer\*, Shu-I Tu, An-Fei Hsu, and Christopher E. Thomas

Plant and Soil Biophysics Research Unit, Eastern Regional Research Center, U.S. Department of Agriculture, Agricultural Research Service, Philadelphia, Pennsylvania 19118

## ABSTRACT

Proton transport by the nitrate-insensitive, vanadate-sensitive ATPase in KI-washed microsomes and reconstituted vesicles from maize (*Zea mays* L.) roots was followed by changes in acridine orange absorbance in the presence of either KNO<sub>3</sub> or KCl. Data from such studies obeyed a kinetic model in which net proton transport by the pump is the difference between the rate of proton transport by the action of the ATPase and the leak of protons from the vesicles in the direction opposite from the pump. After establishing the steady state proton gradient, the rate of return of transported protons was found to obey first-order kinetics when the activity of the ATPase was completely and rapidly stopped. The rate of return of these protons varied with the quencher used. When the substrate Mg:ATP was depleted by the addition of either EDTA or hexokinase, the rate at which the proton gradient collapsed was faster than when vanadate was used as the quencher. These trends were independent of the anion accompanying the K and the transport assay used.

Membranes from maize roots have been shown to contain at least two proton transporting ATPases (6, 28). One of these pumps is localized on the tonoplast membrane and is similar to other vacuolar type ATPases being inhibited by NEM and nitrate, but insensitive to vanadate (7, 28). The other pump is believed to be localized on the plasma membrane and similar to other E1-E2 type ATPase in forming an aspartyl phosphate intermediate, being sensitive to vanadate and utilizing Mg-ATP as substrate (1, 4, 6, 7, 25, 28). Transport ATPases of the E1-E2 type have been shown to exist in at least two different conformational states depending on the ligands bound to the enzyme (1, 25). These conformational states have been deduced by changes in susceptibility to proteolytic degradation (19 and references cited therein) and fluorescence of aromatic amino acids within the protein (14, 16) and covalently bound probes (15). It has been postulated that the changes in protein structure are essential for ion movement (25), because the conformation of the E1-E2 type ATPase is affected by binding of transported cation (14).

Characterization of proton transport by the vanadate-sensitive pump from maize roots has been slowed because of difficulties in purifying plasma membranes with competent transport activities. Problems in isolating these membranes arise from the abundance of proteases in membrane fractions (8) and the presence of lipolytic activities which affect membrane integrity (3). Recent advances in purification of membranes from roots have allowed isolation of vesicles with

vanadate-sensitive proton transport (6, 7, 10). Additionally, several reconstitution protocols have been developed to insert the vanadate-sensitive ATPase into liposomes (3, 26).

In a recent article (28), a kinetic model for describing proton transport by the tonoplast ATPase was proposed. This model quantifies the overall process of proton transport by simultaneously considering the pumping and the leakage of protons from membrane vesicles. This report extends the use of this model to characterize the activity of the vanadate-sensitive proton pump.

## MATERIALS AND METHODS

### Preparation of Membrane Vesicles

Microsomes washed with 0.25 M KI were prepared from roots of 3-d-old maize seedlings (cv WF9 × Mo17) as described previously (3). Vanadate-sensitive proton transport from KI-washed microsomes was reconstituted into liposomes as described previously, except 10 mg of dioleoylphosphatidylcholine and 2 mg of phosphatidylglycerol were used per mg of protein instead of asolectin (3). Characteristics of these reconstituted vesicles were essentially the same as reported previously for the ATPase reconstituted into asolectin vesicles (3). Protein content was determined after deoxycholate-TCA precipitation by the Lowry method (2).

### Proton Transport Assay

Proton transport was followed by changes in the absorbance of AO at 492 nm as described by de Michelis *et al.* (6). Typically, 100 to 200  $\mu$ L of vesicles were diluted with 2 mL of 17.5 mM Mes-BTP<sup>1</sup> (pH 6.45), 25 mM D-glucose, 2.5 mM MgSO<sub>4</sub>, 1 mM EGTA, 7.5  $\mu$ M AO, and 50 mM KNO<sub>3</sub>. After equilibration at 18 to 20°C for 5 min, the reaction was initiated by the addition of 20  $\mu$ L of 0.2 M ATP titrated to pH 6.45 with BTP. Where indicated, proton transport was followed by changes in the fluorescence of AO using excitation and emission wavelengths of 470 and 535 nm, respectively. Results with AO were confirmed by assaying proton uptake by changes in the fluorescence of 10  $\mu$ M quinacrine in the reac-

<sup>1</sup> Abbreviations: BTP, Bis-Tris-Propane; AO, acridine orange; HK, hexokinase;  $k_1$ , rate constant for processes that hinder the build-up of a pH gradient;  $k_2$ , rate constant for return of transported protons after the ATPase has been stopped;  $m$ , the coupling factor relating the rate of ATP hydrolysis to the rate of proton transport;  $R$ , rate of ATP hydrolysis;  $R_H$ , initial rate of proton transport;  $\delta$ , the number of protons transported; subscripts  $o$  and  $s$  following  $\delta$  and  $R$  denote initial and steady state values, respectively.

tion media using excitation and emission wavelengths of 425 and 508 nm, respectively.

### Kinetic Model for Proton Transport

The formation of a proton gradient by a pump usually follows a rather complex time course with the net rate of transport approaching zero after some period of time (28). The decrease in net transport can be attributed to a decline in ATP hydrolysis due to a back-pressure effect in tightly coupled systems (29, 30). Alternatively, the decrease in transport can be accounted by the pump slipping in poorly coupled systems which represent a failure on the molecular events that result in proton movement (21, 22). Additionally, the loss of protons due to leakage tends to increase as the gradient becomes larger, decreasing net pumping. Mathematical treatment of the processes that hinder proton transport in reconstituted purple membranes has been addressed previously (24, 27). This treatment has recently been extended to the ATP-dependent proton pump from maize tonoplast vesicles (28). Net proton pumping at a given time during the formation of a gradient may be represented by

$$(d\delta/dt) = m \cdot R - (k_L + k_{bp}) \cdot \delta = mR - k_1 \delta \quad (1)$$

in which  $\delta$  is the net amount of protons transported across the membrane at time,  $t$ , after the pump is activated by the addition of ATP. Changes in either absorbance or fluorescence of dyes, like quinacrine and AO, can be related directly to the number of protons transported after considering the distribution of the dye and the buffering capacity of the intravesicular space (20). The quantity  $m$  is a measure of the coupling between ATP hydrolysis and proton transport. The rate constants,  $k_L$  and  $k_{bp}$ , represent the membrane leakage during pumping and the back pressure effect, respectively. Inhibition of the buildup of a proton gradient,  $k_1$ , is the sum of these two rate constants.

At steady state, the net rate of proton pumping,  $d\delta/dt$ , approaches zero and therefore,

$$m \cdot R_s = k_1 \cdot \delta_s \quad (2)$$

where the subscript  $s$  denotes the steady state level. If ATP hydrolysis remains unchanged, initial rate of ATP hydrolysis can be substituted for  $R_s$ . Application of steady state approximation yields:

$$m \cdot R_s = m \cdot R_o = m \cdot R = k_1 \cdot \delta_s \quad (3)$$

where the subscript  $o$  denotes initial rate, and reduces Equation 1 to:

$$d\delta/dt = k_1 \cdot (\delta - \delta_s) \quad (4)$$

Upon integration of Equation 4, the following is obtained:

$$\ln(1 - \delta/\delta_s) = -k_1 \cdot t \quad (5)$$

Therefore, Equation 5 provides a convenient means of estimating  $k_1$ , the rate constant that accounts for the reduction in net proton transport due to back-pressure effect and proton leakage, by constructing the semi-log plot of 1 minus (the decrease in absorbance of AO at time  $t$  after the addition of ATP)/(the decrease in absorbance of AO once a steady state value is attained) as a function of time after ATP addition.

Since  $m \cdot R$  is equivalent to the initial rate of proton transport,  $R_H$ , a simple equation for the initial rate of proton transport can be constructed from Equation 3 as follows:

$$R_H = k_1 \cdot \delta_s \quad (6)$$

After a proton gradient is established, its collapse can be induced by the addition of protonophores or inhibitors of ATP hydrolysis. The return of transported protons,  $\delta$ , may be assumed to obey a first-order kinetics,

$$(d\delta/dt) = k_2 \cdot \delta \quad (7)$$

where  $k_2$  is the first-order rate constant for membrane leakage when the pump is not active. Integration of Equation 7 yields:

$$\ln(\delta/\delta_s) = k_2 \cdot t \quad (8)$$

where  $t$  is the time after the pump has been inhibited.

### ATP Hydrolysis Assays

ATP hydrolysis was assayed using 5 to 10  $\mu\text{L}$  of vesicles diluted to 100  $\mu\text{L}$  with reaction media for assaying proton transport without AO. The amount of inorganic phosphate released was determined by the formation of the malachite green-molybdate complex after terminating the reaction with the addition of 100  $\mu\text{L}$  of ice-cold 5% TCA and incubating on ice (28). Alternatively, the rate of ATP hydrolysis was determined by changes in absorbance at 340 nm following the oxidation of NADH in the presence of pyruvate kinase, lactate dehydrogenase and PEP as described previously (28).

## RESULTS AND DISCUSSION

### Kinetics of Proton Transport by Vanadate-Sensitive ATPase

When KI-washed microsomes were supplied with Mg-ATP in the presence of 50 mM  $\text{KNO}_3$ , the absorbance of AO at 492 nm decreased consistent with the transport of protons to the intravesicular space (Fig. 1D, left). These KI-washed microsomes exhibited mostly vanadate-sensitive proton transport. Approximately 80% of the ATP-dependent proton transport by KI-washed microsomes was inhibited by 0.2 mM vanadate in the presence of 50 mM  $\text{KNO}_3$ . There was either no or only slight stimulation of proton transport when  $\text{KNO}_3$  was replaced with KCl, indicating minimal contamination by the tonoplast ATPase (data not shown). The presence of 50 mM  $\text{KNO}_3$  in the reaction media eliminated any possible nitrate-sensitive proton transport remaining after the KI treatment. Similar results were found when the vanadate-sensitive ATPase in KI-washed microsomes was reconstituted into proteoliposomes (Fig. 1D, right). The reconstituted vesicles are a more desirable system to study the vanadate-sensitive ATPase because: (a) nearly all of the ATP hydrolyzing activity is vanadate-sensitive (3); (b) there is no contamination from the nitrate-sensitive proton pump (3); (c) liposomes produced by the reconstitution protocol exhibited low rates of proton leakage when assayed by pH pump experiments (3); and (d) KI-wash microsomes can be stored up to a month at  $-20^\circ\text{C}$  prior to reconstitution and yield proteoliposomes with similar rates of proton transport (data not shown).

To test the effects of three potential quenchers of the

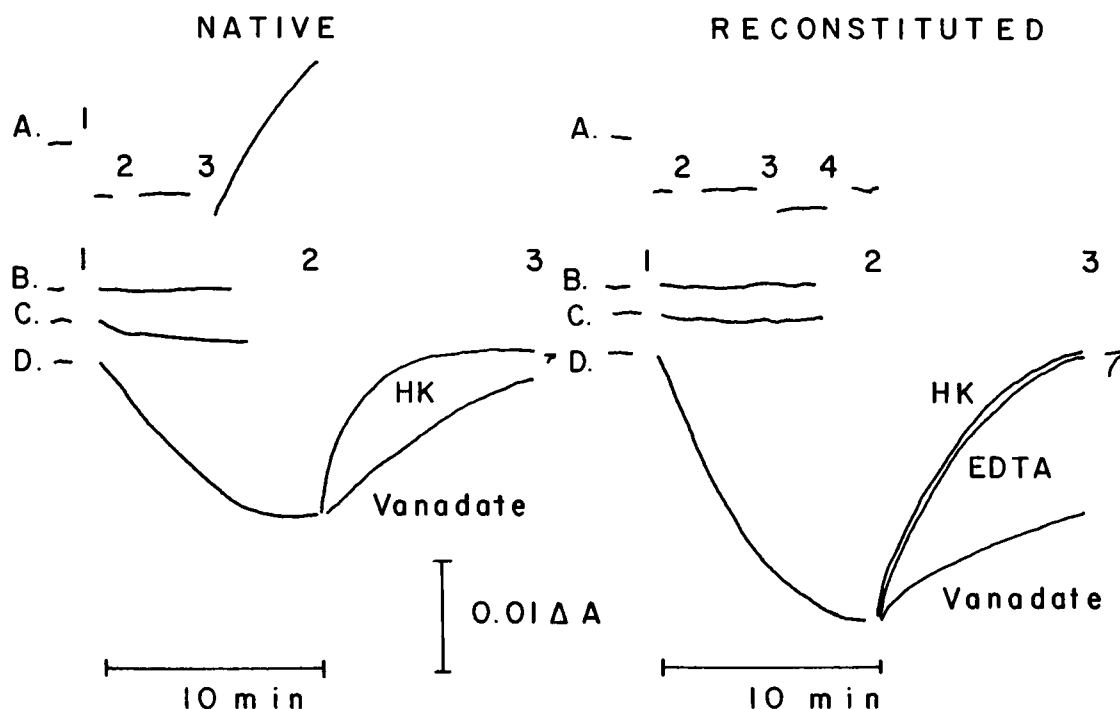


**Figure 1.** Changes in the absorbance of acridine orange at 492 nm as a function of different additives. Native and reconstituted vesicles contained approximately 0.075 mg of protein each in 2.0 mL total volume. A: 50  $\mu$ L of 10 mM sodium vanadate, 100 units of HK in 100  $\mu$ L, 45  $\mu$ L of 0.5 M EDTA, and 20  $\mu$ L of 1 M  $\text{NH}_4\text{Cl}$  were added at points 1, 2, 3, and 4, respectively. B: 20  $\mu$ L of 0.2 M ADP (titrated to pH 6.45 with BTP) was added at point 1. C: The assay medium contained 0.4 mM sodium vanadate and 20  $\mu$ L of 0.2 M ATP was added at point 1. D: 20  $\mu$ L of 0.2 M ATP was added at point 1. At point 2, various inhibitors were added. Inhibitors included 100 units of HK in 100  $\mu$ L and final concentrations of 0.4 mM vanadate and 10 mM EDTA. At point 3, the remaining proton gradient was dissipated by adding 20  $\mu$ L of 1 M  $\text{NH}_4\text{Cl}$ .

ATPase activity, HK, EDTA and vanadate, on the absorbance at 492 nm, each agent was added to vesicles in reaction medium without ATP (Fig. 1). Upon addition of both HK and vanadate to native vesicles, there was only a slight change in absorbance. However, upon addition of EDTA (titrated to pH 6.5 with BTP) to a final concentration of 10 mM, the absorbance at 492 nm increased in a time-dependent fashion. Additionally, absorption spectra of the reaction medium at various times after EDTA addition suggested that the increase in absorbance at 492 nm was due to an increase in light scattering (data not shown), indicative of membrane fusion. Therefore, HK and vanadate were potentially useful quenchers of the ATPase with native vesicles, whereas EDTA was not. With reconstituted vesicles, all three quenchers were potentially useful because they did not induce a time-dependent change in absorbance (Fig. 1).

To improve the quantification of the kinetics of proton transport of the vanadate-sensitive proton pump, it was necessary to determine if changes in AO absorbance conformed to the model previously employed for the tonoplast ATPase (28). One of the prerequisites for the application of this model is that the rate of ATP hydrolysis is constant over time. Interpretation of results of ATP hydrolysis by native vesicles was complicated by the presence of other ATP utilizing enzymes. Using a reaction time of 10 min, Mg-dependent ATP hydrolysis by native and reconstituted vesicles was completely inhibited between 0.2 and 0.4 mM vanadate (Fig. 2). ATP hydrolysis by both native and reconstituted vesicles was linear for at least 15 min (Fig. 3). Mg-dependent ATP hydrolysis

also was linear for 15 min. The Mg-dependent activity was nearly abolished by 0.2 mM vanadate. These results suggested that the E1-E2 type of transport ATPase constituted a vast majority of the Mg-dependent ATP hydrolyzing activity. ATP hydrolysis not inhibited by vanadate was independent of the presence of Mg (Fig. 3), consistent with the notion that this activity did not result from the ATPase. Using the coupled enzyme assay, maximal inhibition of ATP hydrolysis was found 30 to 40 s after the addition of vanadate. The time

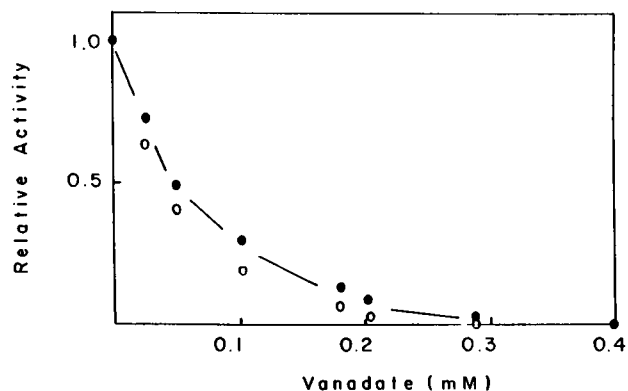


**Figure 2.** Effect of vanadate concentration on Mg-dependent ATP hydrolysis by native and reconstituted vesicles. Activity in the presence and absence of vanadate was determined by the malachite green assay using a reaction time of 10 min. Activity of native ( $\bullet$ ) and reconstituted ( $\circ$ ) vesicles average 52 nmol/min/mg protein in the absence of vanadate.

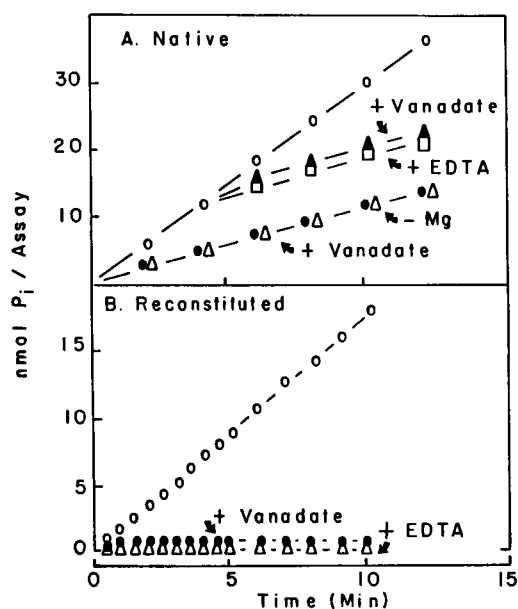


**Figure 3.** Inhibition of ATP hydrolysis by 10 mM EDTA and 0.2 mM vanadate with native (A) and reconstituted (B) vesicles. ATP hydrolysis measured either in the presence of EDTA or the absence of Mg was determined by the malachite green assay. In the other instances, the coupled enzyme assay was used. Assays contained 0.040 and 0.036 mg protein for native and reconstituted vesicles. Assays were initiated by the addition of vesicles. In panel A, assays conducted from time 0 in the presence of vanadate and absence of Mg are represented by (●) and (Δ), respectively. After 4 min, 0.2 mM vanadate (▲) and 10 mM EDTA (□) were added. In both panels A and B, controls are represented by (○). In panel B, assays conducted from time 0 in the presence of 0.2 mM vanadate and 10 mM EDTA are represented by (●) and (Δ), respectively.

course of ATP hydrolysis and inhibition by vanadate was easier to assess with reconstituted vesicles because there was negligible phosphatase activity (3), and similar results were found.

Addition of 10 mM EDTA appeared to completely quench Mg-dependent ATP hydrolysis by native and reconstituted vesicles without a time lag (Fig. 3). The more sensitive coupled enzyme assay could not be used in this instance because the EDTA would remove divalent cations required for pyruvate kinase (12), one of the constituents of the assay medium.

Another prerequisite for the application of the model is that the initial rate of proton transport was related to the rate of ATP hydrolysis. Rates of nitrate-insensitive, vanadate-sensitive proton transport and ATP hydrolysis by both native and reconstituted vesicles exhibited a similar dependence on ATP concentration (Fig. 4). The  $K_m$  for ATP averaged 0.4 mM for the four different activities (data not shown).

When data concerning changes in AO absorbance by KI-washed microsomes were transformed, a plot of  $\ln(1 - \delta/\delta_s)$  as a function of time yielded a straight line (Fig. 5A). Data in the changes in absorbance of AO by reconstituted vesicles also obeyed the above relationship. Therefore, proton transport by the vanadate-sensitive ATPase in both native and reconstituted vesicles apparently obeyed a model that represents net proton transport as the difference between proton pumping and factors contributing to back-pressure effects and proton leakage from the vesicles. ATP hydrolysis by both

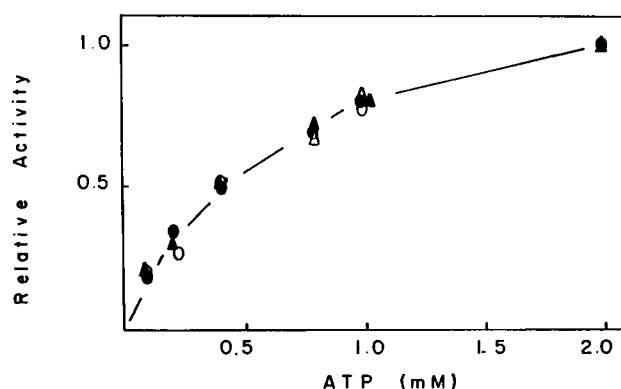


**Figure 4.** Effect of ATP concentration on the rates of vanadate-sensitive ATP hydrolysis and nitrate-insensitive proton transport. ATP hydrolysis at 2 mM concentration averaged 56 nmol Pi/min/mg protein for both native (●) and reconstituted vesicles (○). Proton transport averaged 0.08 and 0.11  $\Delta A$ /min/mg protein for native (▲) and reconstituted (Δ) vesicles.

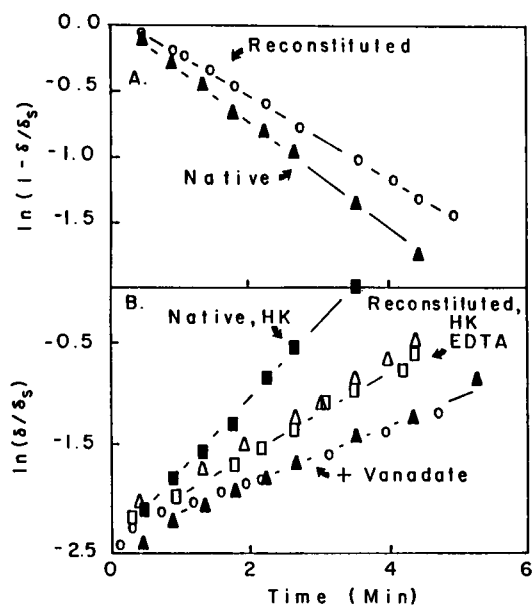


**Figure 5.** Changes in acridine orange absorbance during the buildup and collapse of proton gradient. Data from the build (A) and collapse (B) of pH gradients were transformed and plotted according to Equations 5 and 8, respectively, in "Materials and Methods." Data from native and reconstituted vesicles in A are represented by closed and open symbols, respectively. Data from the collapse of pH gradients was induced by HK (■ and □ with native and reconstituted vesicles, respectively), vanadate (▲ and ○ with native and reconstituted vesicles, respectively) and EDTA with reconstituted vesicles only (Δ). Data from the collapse of the proton gradient with native vesicles by HK was displaced + 0.5 units along the Y intercept for clarity, hydrolysis, and nitrate-insensitive proton transport.

native and reconstituted vesicles did not diminish as proton transport attained a steady state gradient (Figs. 1 and 3). ATP hydrolysis was linear for at least 15 min, whereas proton transport attained a steady state gradient within this time. Thus, the reduction in net proton transport was not due to thermodynamic inhibition and the contribution of a back-pressure effect to  $k_1$  was small. Therefore,  $k_1$  is primarily an estimate of proton leakage during the buildup of the proton

gradient and the outward leakage of protons during the pumping phase,  $k_1$ , can be estimated from the slope of the  $\ln(1-\delta/\delta_s)$  versus time. The slopes of such plots ( $k_1$ ) for native and reconstituted vesicles differed slightly with native vesicles being greater.

To estimate  $k_2$ , the membrane permeability to protons when the pump is not catalyzing transport, the proton transport is allowed to proceed until a steady state AO absorbance was achieved, at which point ATP hydrolysis was stopped and the loss of the proton gradient was followed. Under these conditions, the increase in absorbance of AO should obey a first-order kinetics, *i.e.* a plot of  $\ln(\delta/\delta_s)$  as a function of time should be a linear relationship. Quenchers employed in these studies must satisfy two requirements: (a) they should not alter the absorbance of the reaction media at 492 nm, and (b) they should ATP hydrolysis completely and rapidly. The effects of all three potential quenchers, vanadate, EDTA, and HK, on absorbance at 492 nm and the ability of vanadate and EDTA to rapidly inhibit the ATPase have been demonstrated above. The ability of HK to remove ATP from the assay solution was determined by adding HK to 2 mM ATP solution in the presence of the coupled enzyme reaction media and following changes in absorbance at 340 nm as a function of time after HK addition. The addition of 100 units of HK completely depleted the ATP in 2 mL of a 2 mM solution within 10 s (data not shown). Thus, all three compounds appeared to quench the vanadate-sensitive ATPase within a minute after addition, with HK and EDTA being almost instantaneous.

When the ATPase was inhibited by the addition of vanadate, the proton gradient dissipated rather slowly as evident by the slow increase in absorbance at 492 nm (Fig. 1). When the data were transformed and plotted as a first-order reaction rate (Fig. 5B), the proton gradient initially dissipated at a relatively fast rate, but slowed to a constant rate after about 40 s as evident by the linear relationship between  $\ln(\delta/\delta_s)$  and time. The proton gradient dissipated at a much faster rate after the addition of HK. With native vesicles, the slopes of the first-order reaction plot were about 2.4 times as great in the presence of HK than in the presence of vanadate (Table I). The rate of proton leakage when ATP hydrolysis of native vesicles was stopped by HK,  $k_2$ , was similar to the rate of collapse of an imposed pH gradient in pH jump experiments reported previously (3). Equivalent results were found when proton transport by reconstituted vesicles was arrested (Table I). The collapse of proton gradients generated by the ATPase after the addition of inhibitors conformed to first-order kinetics (Fig. 3) with the leakage rate of protons being 1.7 times greater after the addition of HK as compared to vanadate (Table I). When ATP hydrolysis was arrested by EDTA, the gradient dissipated at a rate comparable to that found with HK (Table I).

Both EDTA and HK quenched the enzyme by removing its substrate, Mg:ATP, whereas vanadate probably forms an intermediate analog (17), thereby inhibiting ATPase activity. Binding of Mg:ATP alters the conformational state of E1-E2 type ATPases (14, 15, 19). The structure of the vanadate-complexed enzyme is also different from that of the unliganded enzyme (19, 25). Although little is known about the conformational states of the vanadate-sensitive ATPase from

maize root microsomes, it is likely that its reaction mechanism involves distinct protein configurations like other E1-E2 ATPases. Thus, the difference in proton leakage from vesicles when the ATP hydrolysis was arrested by substrate depletion versus that by vanadate may reflect differences in the mode of inhibition of these compounds. Recently, duPont *et al.* (7) reported vanadate inhibited the initial rate of proton transport more than the extent of transport. Differences in the rates of proton diffusion during the buildup and collapse of a proton gradient generated by a proton pump have been reported previously for other transporters (27 and references cited therein).

In a similar study with the vanadate-sensitive proton pump from *Neurospora*, Perlin *et al.* (20) concluded that the rate of proton leakage after ATP hydrolysis was stopped was independent of the arresting agent. In light of our results, a closer examination of these earlier results seems to be warranted. In Perlin's *et al.* work, when the ATP hydrolysis was stopped by either the addition of 3 mM EDTA or HK plus glucose, the rate of proton leakage was  $176 \pm 6$  and  $172 \pm 10$  relative units/min. Upon inhibition by vanadate, the rate was less,  $144 \pm 11$  relative units/min. Therefore, similar results may have been obtained by Perlin *et al.* (20) with the *Neurospora* enzyme, although the magnitude of the difference between arresting agents was not as great as reported here.

To determine if the enhanced proton leakage associated with substrate depletion of the ATPase is progressive with declining substrate levels, the effect of ATP concentration on the rate of proton leakage during the buildup of the proton gradient,  $k_1$ , was evaluated. These analyses indicated that proton leak during pumping,  $k_1$ , increased when the ATP concentration was decreased below 0.2 mM (Fig. 6). The other two kinetic parameters, initial rate of proton transport,  $R_H$ , and the extent of proton transport,  $\delta_s$ , had Michealis-Menten like kinetics saturating as the ATP concentration approached 2 mM. The lines for native and reconstituted vesicles extrapolated to the Y axis, 0 mM ATP, at approximately the same rate of proton leakage as when the ATP hydrolysis was stopped by either HK or EDTA addition.

### Effect of Assay Conditions on $k_1$ and $k_2$

Recently, Pope and Leigh (23) summarized a series of experiments indicating that in the presence of nitrate, AO induced an increase in the membrane's permeability to protons. The kinetics of proton transport in the presence of  $\text{KNO}_3$  were compared to that in KCl to determine if a similar phenomenon occurred in our systems and whether the relatively high rates observed for  $k_1$  and  $k_2$  stemmed from our use of AO and  $\text{KNO}_3$ . Unequivocal results could not be obtained with many preparations of native vesicles since they contained traces amounts of nitrate-sensitive proton pump. The activity from this second pump would interfere with the measurements of the activity of the vanadate-sensitive proton pump made in the presence of KCl. However, about one preparation of the KI-washed microsomes out of five lacked the nitrate-sensitive proton pump as evident by the absence of proton transport activity in the presence of 50 mM KCl and 0.2 mM vanadate. With such preparations of KI-washed vesicles, proton transport was not as great in the presence of chloride as compared to nitrate. The initial rate of proton transport was

**Table 1.** Summary of Kinetic Parameters Describing Proton Transport by the Vanadate-Sensitive Proton Pump in Native and Reconstituted Vesicles

Data from changes in either absorbance or fluorescence of either acridine orange or quinacrine were transformed as described in "Materials and Methods" to yield the following kinetic parameters: steady state change ( $\delta_s$ ), rate of proton leakage during pumping ( $k_1$ ), initial rate of proton pumping ( $R_o$ ), and the rate of proton leakage after ATP hydrolysis was stopped ( $k_2$ ).

Assay Conditions	Kinetic Parameters			
	$\delta_s$	$k_1$	$R_o$	$k_2$
	$\text{mg protein}^{-1}$	$\text{min}^{-1}$	$\text{mg protein}^{-1} \text{min}^{-1}$	$\text{min}^{-1}$
Native vesicles				
AO absorbance change				
Buildup of pH gradient	0.145 A	0.414	0.060 A	
Collapsed				
by HK				0.720
by 0.4 mM vanadate				0.386
Reconstituted vesicles				
AO absorbance change				
Buildup of pH gradient	0.332 A	0.346	0.121 A	
Collapsed				
by HK				0.491
by 10 mM EDTA				0.484
by 0.2 mM vanadate				0.233
AO fluorescence change				
Buildup of pH gradient	111.1%	0.298	33.1%	
Collapsed				
by HK				0.451
by 10 mM EDTA				0.400
by 0.2 mM vanadate				0.185
Quinacrine fluorescence change				
Buildup of pH gradient	56.5%	0.340	19.2%	
Collapsed				
by HK				0.476
by 10 mM EDTA				0.431
by 0.2 mM vanadate				0.203

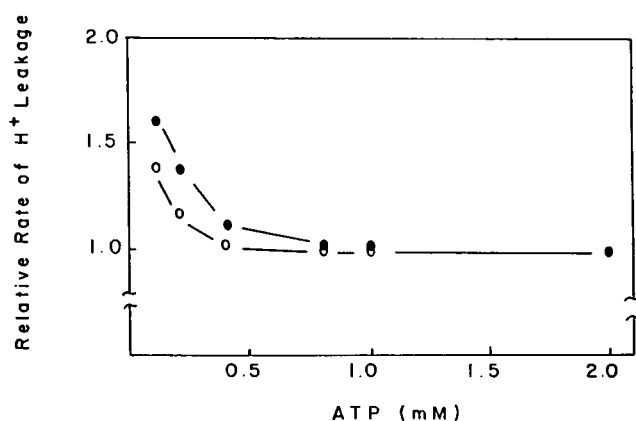


**Figure 6.** Effect of ATP concentration on the leakage of protons during proton pumping,  $k_1$ . Data from Figure 2 for proton pumping by native (●) and reconstituted (○) vesicles were analyzed according to Equation 5 in "Materials and Methods." Values of  $k_1$  for native and reconstituted vesicles at 2 mM ATP averaged 0.41 and 0.32  $\text{min}^{-1}$ , respectively.

0.088 and 0.052  $\Delta\text{A}/\text{min}/\text{mg protein}$  in the presence of nitrate and chloride, respectively, while the extent of change in AO absorbance,  $\delta_s$ , was 0.17 and 0.13  $\Delta\text{A}/\text{mg protein}$ , respectively. Such differences in proton transport by vanadate-sensitive proton pumps have been reported previously (5, 9) and have been explained by differences in the ability of different anions to dissipate the membrane potential created by the electrogenic transfer of protons. The rates of proton leakage across the vesicles after the pump was stopped by HK addition,  $k_2$ , were similar in the presence of chloride and nitrate, 0.63 and 0.70  $\text{min}^{-1}$ , respectively. The comparison between KCl and  $\text{KNO}_3$  could readily be made with proteoliposomes because the nitrate-sensitive proton pump is not recovered during reconstitution (3). The lack of an effect of KCl and  $\text{KNO}_3$  on the proton leakage rate ( $k_2$ ) of reconstituted vesicles was similar to native vesicles. The rate and extent of proton transport were not as great in the presence of chloride as compared to nitrate. The initial rate of proton transport with reconstituted vesicles was 0.093 and 0.030  $\Delta\text{A}/\text{min}/\text{mg protein}$  in the presence of nitrate and chloride, respectively, while the extent of change in AO absorbance was 0.31 and 0.15  $\Delta\text{A}/\text{mg protein}$ , respectively. The rates of return of transported protons after inhibition of the pump by HK,  $k_2$ , were similar, 0.42 and 0.37  $\text{min}^{-1}$  in the presence of nitrate

and chloride, respectively. The lack of a difference in the rate of proton leakage between chloride and nitrate suggested that nitrate ions were not altering the intrinsic permeability of membranes in the presence of AO. Similarly, duPont *et al.* (7) recently concluded that proton transport by the vanadate-sensitive pump from barley roots could be followed by changes in the spectral properties of AO.

To confirm the results obtained from changes in AO absorbance, proton transport by reconstituted vesicles was followed by changes in the fluorescence of AO and quinacrine (Table I). Essentially the same rate constants for proton leakage during the pumping stage of the assay ( $k_1$ ) and after the addition of arresting agents ( $k_2$ ) were found for the three different assays for proton transport. These results provided further evidence that the results were not confounded by the use of AO and nitrate containing buffers.

#### Estimation of the Stoichiometry of the Vanadate-Sensitive Proton Pump

A tentative stoichiometry for the vanadate-sensitive proton pump was estimated by the following approach. One of the methods for relating changes in the absorbance or fluorescence of a pH dependent probe is to plot the ratio of the intravesicular and extravesicular concentration of the probe as a function of imposed pH gradients (20). For such a correlation one needs to know the internal volume of the vesicles. The internal volume was determined both experimentally and empirically. When liposomes were chromatographed on a Sepharose CL-2B column, the phospholipids eluted with a retention volume that was slightly less than that of 38 nm diameter latex beads (data not shown). Assuming a bilayer thickness of 0.5 nm and that each phospholipid head occupied 0.5 nm<sup>2</sup> of surface area (13), an internal volume of

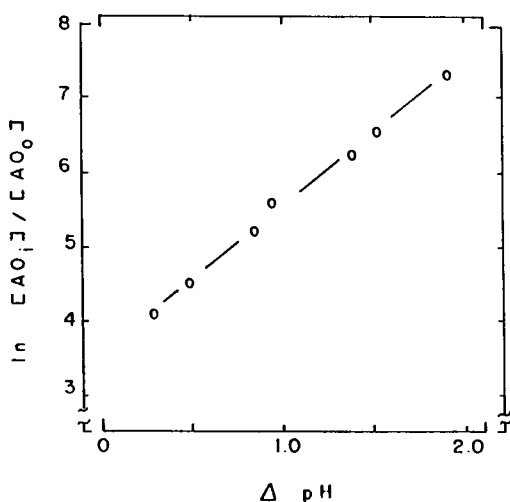


**Figure 7.** Distribution of acridine orange between the intravesicular space and external solution as a function of imposed pH gradient. Reconstituted vesicles formed and equilibrated at various pH values between 4.5 and 6.5 were diluted into reaction medium at pH 6.5. The decrease in absorbance sensitive to  $\text{NH}_4\text{Cl}$  was used to calculate the distribution of acridine orange between the intravesicular space and the external solution assuming the fractional decrease in absorbance represented the fraction of acridine orange taken up by the proteoliposomes (20).

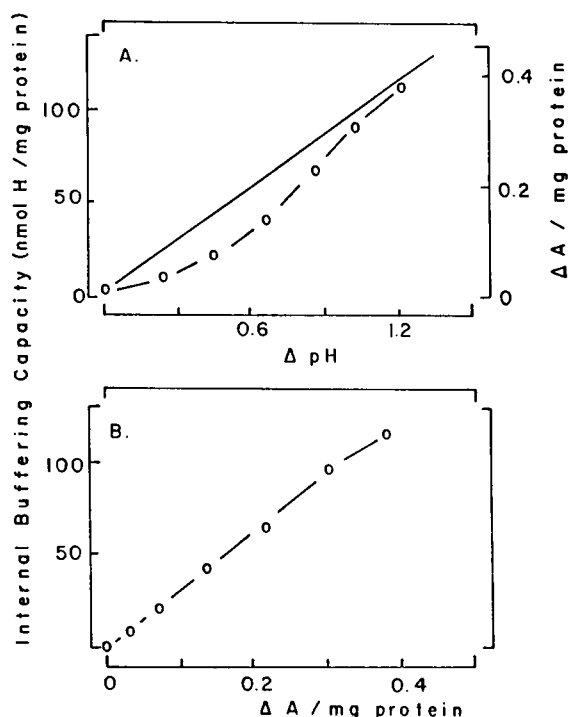


**Figure 8.** Relationship between changes in absorbance of acridine orange and protons within the intravesicular space. A: The changes in AO absorbance as a function of an imposed pH gradient (O) and the number of protons needed to lower the pH of the intravesicular space by 0 to 1.5 units (—) as determined by the method of Ramirez *et al.* (24). B: From the data in panel A, a calibration curve relating changes in AO absorbance and number of protons was constructed.

0.57  $\mu\text{L}/\text{mg}$  of phospholipid was calculated. This empirical value was very close to the value of 0.52  $\mu\text{L}/\text{mg}$  of phospholipid determined experimentally by the amount of carboxyfluorescein trapped by the liposomes during reconstitution according to the method of Goormaghtigh and Scarborough (11). Vesicles were then reconstituted at different pH values from 5 to 6.5. Fifty  $\mu\text{L}$  aliquots were diluted into AO assay media (pH 6.5), and the change in absorbance at 492 nm was monitored. After a few minutes, the remaining pH gradient was collapsed by the addition of 20  $\mu\text{L}$  of 1 M  $\text{NH}_4\text{Cl}$ . Using the above value for the intravesicular volume, the concentration of AO inside and outside of the liposomes was calculated, assuming that the observed decrease in absorbance represented the amount of AO within the vesicles. The logarithm of the intravesicular and extravesicular AO concentration was plotted as a function of the imposed pH buffer (Fig. 7). From this calibration curve, the average  $\delta$ , for the reconstituted pump was found to represent an average pH gradient of 1.1 units. The internal buffering capacity of the liposomes was determined by the method of Maloney (18) after reconstituting the vesicles in 0.15 M KCl. The buffering capacity was found to be relatively constant over the pH range of 4.8 to 6.5 and averaged approximately 100 nmol  $\text{H}^+/\text{pH}$  unit/mg protein. Therefore, the steady state value of  $\delta$ , represented about 110 nmol  $\text{H}^+/\text{mg}$  protein. The coupling factor,  $m$ , was then estimated by the equation  $m \cdot R = k_1 \cdot (\delta_s)$  using an average rate of vanadate sensitive ATP hydrolysis of 50 nmol/min/

mg protein, and a  $k_1$  value of  $0.36 \text{ min}^{-1}$ , the coupling factor,  $m$ , or transport stoichiometry, was found to be 0.8.

One of the assumptions of the model of Tu *et al.* (28) is that the change in absorbance of AO is linearly related to the number of transported protons. Therefore, the use of an alternative calibration curve was tested. Changes in absorbance of AO were plotted as a function of imposed pH gradient (Fig. 8). Also, the number of nmol of  $\text{H}^+$  necessary to change the pH of the intravesicular space was estimated by titrating vesicles in the presence and absence of 0.02% Triton X-100 following a protocol similar to Ramirez *et al.* (24). This difference was plotted as a function of the change in pH. Using these data, a plot of the change in AO absorbance against the number of protons was constructed, which was relatively linear. Using this type of calibration, a similar value for the stoichiometry for the vanadate-sensitive proton pump was obtained, 0.8. These results suggest that the vanadate-sensitive proton pump from maize root microsomes may be very similar to that of *Neurospora* which has been found to have a stoichiometry of proton transport to ATP hydrolysis of 1.0 (20).

#### LITERATURE CITED

- Amory A, Goffeau A, McIntosh DB, Boyer PD (1984) Contribution of  $^{18}\text{O}$  to the mechanism of the  $\text{H}^+$ -ATPase from yeast plasma membranes. *Curr Top Cell Regul* 24: 471–483
- Bensadoun A, Weinstein D (1976) Assay of proteins in the presence of interfering materials. *Anal Biochem* 70: 241–250
- Brauer D, Hsu A-F, Tu S-I (1988) Factors associated with the instability of nitrate-insensitive proton pumping by maize root microsomes. *Plant Physiol* 87: 598–602
- Briskin DP (1986) Intermediate reaction states of the red beet plasma membrane ATPase. *Arch Biochem Biophys* 248: 106–115
- Calahorra M, Rasmirez J, Clemente SM, Pena A (1987) Electrochemical potential and ion transport in vesicles of yeast plasma membrane. *Biochim Biophys Acta* 899: 229–238
- de Michelis MI, Spanswick RM (1986)  $\text{H}^+$ -pumping driven by the vanadate-sensitive ATPase in membrane vesicles from corn roots. *Plant Physiol* 81: 542–547
- Dupont FM, Tanaka CK, Hurkman WJ (1988) Separation and immunological characterization of membrane fractions from barley roots. *Plant Physiol* 86: 717–724
- Gallagher SR, Carroll EJ, Leonard RT (1986) A sensitive diffusion plate assay for screening inhibitors of protease activity in plant cell fractions. *Plant Physiol* 81: 869–874
- Giannini JL, Briskin DP (1987) Proton transport in plasma membrane and tonoplast vesicles from red beet (*Beta vulgaris* L.) storage tissue. A comparative study of ion effects on  $\text{pH}$  and  $\text{u}$ . *Plant Physiol* 84: 613–618
- Giannini JL, Gildensoph LH, Briskin DP (1987) Selective production of sealed plasma membrane vesicles from red beet (*Beta vulgaris* L.) storage tissue. *Arch Biochem Biophys* 254: 621–630
- Goormaghtigh E, Scarborough GA (1986) Density-based separation of liposomes by glycerol gradient centrifugation. *Anal Biochem* 159: 122–131
- Holmsen H, Storm E (1969) The adenosine triphosphate inhibition of the pyruvate kinase reaction and its dependence on the total magnesium ion concentration. *Biochem J* 112: 302–312
- Jain MK, Wagner RC (1980) Introduction to Biological Membranes. John Wiley and Sons, New York, pp 1–382
- Jorgensen PL, Petersen J (1985) Chymotrypsin cleavage of  $\alpha$ -subunit in E1-forms of renal ( $\text{Na}^+ + \text{K}^+$ )-ATPase: effects on enzymatic properties, ligand binding and cation exchange. *Biochem Biophys Acta* 821: 319–333
- Kurtenbach E, Verjovski-Almeida S (1985) Labeling of a thiol residue in sarcoplasmic reticulum ATPase by pyrene maleimide. Solvent accessibility studied by fluorescence quenching. *J Biol Chem* 260: 9636–9641
- Ludi H, Hasselbach W, Gaugler H (1985) Tryptophan fluorescence of sarcoplasmic reticulum ATPase. A fluorescence quench study. *Biochem Biophys Acta* 814: 120–124
- Macara LG (1980) Vanadium—an element in search of a role. *Trends Biochem Sci* 5: 92–94
- Maloney PC (1979) Membrane  $\text{H}^+$  conductance of *Streptococcus lactis*. *J Bacteriol* 140: 197–205
- Perlin DS, Brown CL (1987) Identification of structurally distinct catalytic intermediates of the  $\text{H}^+$ -ATPase from yeast plasma membrane. *J Biol Chem* 261: 6788–6794
- Perlin DS, San Francisco MJD, Slayman CW, Rosen BP (1986)  $\text{H}^+$ /ATP stoichiometry of proton pumps from *Neurospora crassa* and *Escherichia coli*. *Arch Biochem Biophys* 248: 53–61
- Pietrobon D, Azzone GF, Walz D (1981) Effect of funiculosin and antimycin A on the redox-driven  $\text{H}^+$ -pumps in mitochondria: On the nature of leaks. *Eur J Biochem* 117: 389–394
- Pietrobon D, Zoratti M, Azzone GF, Stucki JW, Walz D (1982) Nonequilibrium thermodynamic assessment of redox-driven  $\text{H}^+$  pumps in mitochondria. *Eur J Biochem* 127: 483–494
- Pope AJ, Leigh RA (1987) Is there a nitrate/ $\text{H}^+$  symport at the tonoplast (abstract 674)? *Plant Physiol* 83: S-112
- Ramirez F, Ozazaki H, Tu S-I, Hutchinson H (1983) Proton movement in reconstituted purple membrane of *Halobacterium*: effects of pH and ionic composition of the medium. *Arch Biochem Biophys* 222: 464–472
- Scarborough GA (1985) Binding energy, conformational change and the mechanism of transmembrane solute movements. *Microbiol Rev* 49: 214–231
- Singh SP, Sudershan Kesav BV, Briskin DP (1987) Reconstitution and rapid partial purification of the red beet plasma membrane ATPase. *Physiol Plant* 69: 617–626
- Tu S-I, Hutchinson H (1984) Temperature dependence of light-induced proton movement in reconstituted purple membranes. *Arch Biochem Biophys* 228: 609–616
- Tu S-I, Nagahashi G, Brouillette JN (1987) Proton pumping kinetics and origin of nitrate inhibition of tonoplast-type  $\text{H}^+$ -ATPase. *Arch Biochem Biophys* 256: 625–637
- Westerhoff HV, Hellingwerf KJ, Arents JC, Scholte BJ, Vam Dam K (1981) Mosaic nonequilibrium thermodynamics describes biological energy transduction. *Proc Natl Acad Sci USA* 78: 3554–3558
- Westerhoff HV, Scholte BJ, Hellingwerf KJ (1979) Bacteriorhodopsin in liposomes, I. A description using irreversible thermodynamics. *Biochim Biophys Acta* 547: 544–560